Design of Gd(III)-Based Magnetic Resonance Imaging Contrast Agents: Static and Transient Zero-Field Splitting Contributions to the Electronic Relaxation and Their Impact on Relaxivity

Meriem Benmelouka, Alain Borel, Loick Moriggi, Lothar Helm,* and André E Merbach

Institute of Chemical Sciences and Engineering, Ecole Polytechnique Fédérale de Lausanne, CH-1015 Lausanne, Switzerland

Received: May 30, 2006; In Final Form: November 1, 2006

A multiple-frequency (9.4−325 GHz) and variable-temperature (276−320 K) electron paramagnetic resonance (EPR) study on low molecular weight gadolinium(III) complexes for potential use as magnetic resonance imaging (MRI) contrast agents has been performed. Peak-to-peak linewidths ΔH_{pp} and central magnetic fields have been analyzed within the Redfield approximation taking into account the static zero-field splitting (ZFS) up to the sixth order and the transient ZFS up to the second order. Longitudinal electronic relaxation is dominated by the static ZFS contribution at low magnetic fields ($B < 0.3$ T) and by the transient ZFS at high magnetic fields ($B > 1.5$ T). Whereas the static ZFS clearly depends on the nature of the chelating ligand, the transient ZFS does not. For the relatively fast rotating molecules studied water proton relaxivity is mainly limited by the fast rotation and electronic relaxation has only a marked influence at frequencies below 30 MHz. From our EPR results we can conclude that electronic relaxation will have no influence on the efficiency of Gd(III)-based MRI contrast agents designed for studies at very high magnetic fields ($B > 3$T).

Introduction

Magnetic resonance imaging (MRI) has a number of important advantages over other noninvasive imaging modalities: It has high spatial resolution (when compared with, for example, positron emission tomography), it has very good sample penetration (when compared with optical imaging methods), and it is already widely used in the clinic. A drawback is its low sensitivity compared with other methods, and therefore powerful signal amplification and contrast enhancement strategies are required. One of these strategies led to the development of paramagnetic contrast agents, mainly gadolinium(III) complexes. The design of new, more efficient Gd(III)-based MRI contrast media requires the complete understanding of all factors and mechanisms that influence proton relaxivity, i.e., the efficiency of such complexes.[1,2] Proton relaxivity (r_1) is defined as the increase of the longitudinal water proton relaxation rate per millimolar concentration of Gd(III). The relaxivity can theoretically be increased to over 100 mM^{-1} s^{-1} for monohydrated Gd(III) chelates instead of $r_1 = 4-5$ mM^{-1} s^{-1} for the current commercial agents.[2] The maximum proton relaxivity for Gd(III) complexes is expected when the four most important influencing factors are simultaneously optimized: (1) the exchange rate k_{ex} of the water molecules directly bound to the metal, (2) the hydration number q, (3) the rotational diffusion of the complex, described by a correlation time τ_R, and (4) the electronic spin relaxation times T_{1e} and T_{2e}. While the molecular factors influencing the three first parameters are rather well understood, the longitudinal and transverse electronic relaxation of the Gd(III) complexes remains the subject of much discussion.[3−5] In recent years a variety of chelating ligands have been synthesized leading to stable Gd(III) complexes with hydration numbers $q \geq 1$ and optimized water exchange rates k_{ex}.

These low molecular weight complexes are prime candidates as building blocks for the development of macromolecular high relaxivity contrast agents.[6] Indeed, in the past, the nonoptimal water exchange rate k_{ex} has been a critical issue for macromolecular Gd(III)-based MRI contrast agents, since low exchange rates often limit proton relaxivity.[7,8] In view of obtaining independent information on parameters governing electronic relaxation, an extensive multiple-frequency (9.4−325 GHz) and variable-temperature (276−350 K) EPR study has been performed on a variety of Gd(III) complexes with acyclic, macrocyclic, and cryptand ligands.

The acyclic ligands (Scheme 1) used in our study are obtained by either replacing one acetate arm by a propionate moiety ([Gd(DTTA-prop)$(H_2O)]^{2-}$)[11] or elongating one of the ethylene bridges of the diethylenetriamine backbone ([Gd(EPTPA)$(H_2O)]^{2-}$ and [Gd(EPTPA-BAA)(H_2O)]).[6,11] All three complexes show water exchange rates that are largely enhanced compared to the commonly used [Gd(DTPA)$(H_2O)]^{2-}$.

Two different classes of complexes formed with macrocyclic ligands have been chosen for our EPR study. The first one is based on the DOTA ligand; by replacing one and two ethylene bridges by propylene bridges, the TRITA and TETA ligands were produced, respectively (Scheme 2).[9] These modifications lead in the case of [Gd(TRITA)$(H_2O)]^-$ to an increase of k_{ex} by 2 orders of magnitude as compared to [Gd(DOTA)$(H_2O)]^-$, and in the case of $[Gd(TETA)]^-$ to the elimination of the water molecule from the first coordination shell. The second class, also based on the DOTA ligand, is formed of ligands with a phosphinate group replacing one carboxylate (Scheme 3).[12] The water exchange rates for these [Gd(DO3APEt)$(H_2O)]^-$ and [Gd(DO3APEt_2)(H_2O)] complexes are only slightly enhanced

* Author to whom correspondence should be addressed. Fax : (+41) 21-693-9875. E-mail: lothar.helm@epfl.ch.

10.1021/jp0633289 CCC: $37.00
Published on Web 01/09/2007

SCHEME 1: Molecular Structures of the Acyclic Ligands

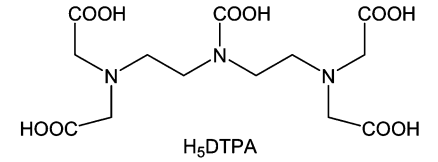

H_5DTPA

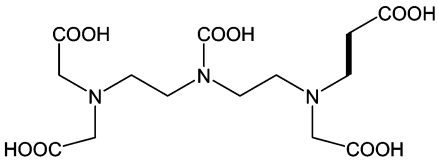

H_5DTTA-Nprop

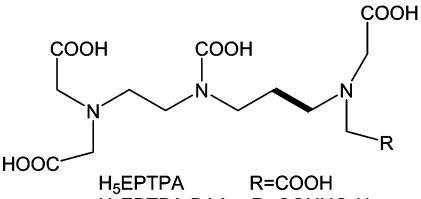

H_5EPTPA R=COOH
H_5EPTPA-BAA R=$CONHC_5H_{11}$

SCHEME 2: Molecular Structures of the Macrocyclic DOTA-Type Ligands

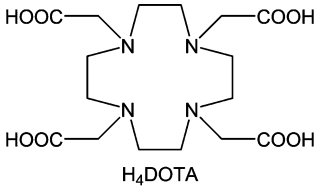

H_4DOTA

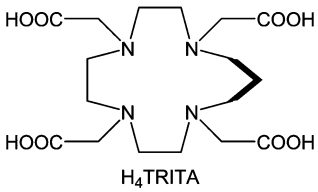

H_4TRITA

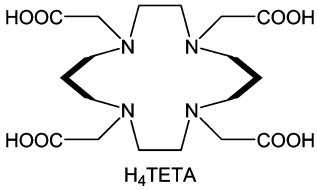

H_4TETA

compared to $[Gd(DOTA)(H_2O)]^-$. However, they provide increased ^{1}H relaxivity due to the presence of second shell water molecules.

Another possible route for higher relaxivity is to increase the hydration number q. The cryptand ligands CTBP and CTBPMe form Gd(III) complexes with three water molecules in the first coordination sphere (Scheme 4). The k_{ex} values for the positively charged complexes $[Gd(CTBP)(H_2O)_3]^{3+}$ and $[Gd(CTBPMe_2)(H_2O)_3]^{3+}$ are of the same order as those of the DTPA and DOTA complexes, but the observed relaxivities are more than twice as much (at 20 MHz) due to $q = 3$.[13]

In this paper, we report the analysis of multifrequency variable-temperature EPR spectra with the Rast−Fries model

SCHEME 3: Molecular Structures of the Macrocyclic Ligands Containing Phosphinate Groups

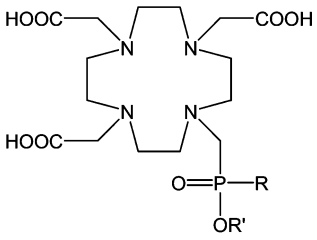

H_3DO3APEt R = Et R' = H
H_3DO3APEt$_2$ R = Et R' = Et

SCHEME 4: Molecular Structures of the Cryptands

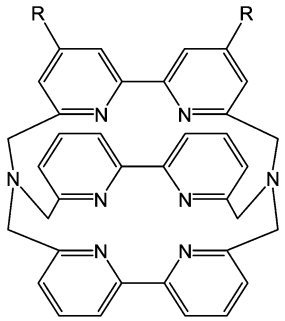

CTBP R = H
CTBPMe R = $COOCH_3$

and discuss the influence of electron spin relaxation on the water proton relaxivity.

Electron Spin Relaxation and Water Proton Relaxivity

Before presenting the EPR results on several low molecular weight gadolinium complexes we will discuss the relevance of electron spin relaxation to water proton relaxivity, r_1. At magnetic fields relevant for MRI (0.47−3.0 T, corresponding to resonance frequencies of 20−128 MHz) water proton relaxivity is mainly governed by the second-order rotational correlation time, $\tau_R^{(2)}$, and the longitudinal electronic relaxation, T_{1e}, assuming $k_{ex} = 10^8\ s^{-1}$. At these magnetic fields the spectral density $J(\omega_I, \tau_{d1})$ is dominating the relaxivity. Figure 1a shows inner sphere proton relaxivities calculated with Solomon−Bloembergen−Morgan (SBM) equations (eqs 1−3) for four different rotational correlation times $\tau_R^{(2)}$. These calculations illustrate the dominance of the $J(\omega_I,\tau_{d1})$ term (dashed lines) and the small contribution due to $J(\omega_S,\tau_{d2})$ (dotted lines)

$$r_1 = \frac{1.8 \times 10^{-5}}{T_{1m} + \tau_m} \tag{1}$$

$$\frac{1}{T_{1m}} = C_{dd}(3J(\omega_I,\tau_{d1}) + 7J(\omega_S,\tau_{d2})) \tag{2}$$

with $C_{dd} = 2/15(\mu_0/4\pi)^2(\gamma_I\gamma_S\hbar r_{IS}^{-3})^2$, $J(\omega,\tau) = \tau/(1 + \omega^2\tau^2)$, $1/\tau_{di} = 1/\tau_2 + 1/T_{ie} + k_{ex}$, and $i = 1,2$

$$\frac{1}{T_{1e}} = \frac{12}{5}(a_{2T})^2\tau_v\left(\frac{1}{1 + \omega_S{}^2\tau_v{}^2} + \frac{4}{1 + 4\omega_S{}^2\tau_v{}^2}\right) \tag{3}$$

The height of the relaxivity hump centered between 30 and 70 MHz strongly depends on the rotational correlation time $\tau_R^{(2)}$: the slower the rotational motion, the higher the relaxivity at these frequencies. The dependence of relaxivity on the

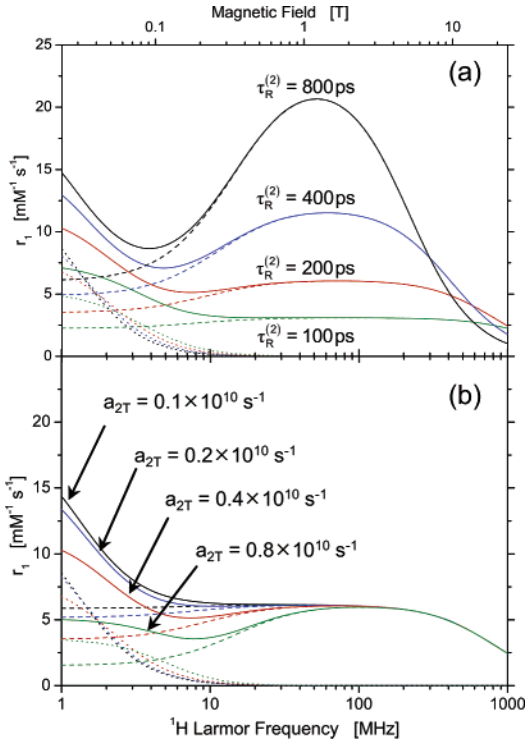

Figure 1. Inner sphere contribution to relaxivity as a function of ^{1}H Larmor frequency calculated with the SBM equations for (a) different rotational correlation times $\tau_R^{(2)}$ ($a_{2T} = 0.4 \times 10^{10}$ s^{-1}) and (b) different transient ZFS strengths a_{2T} ($\tau_R^{(2)} = 200$ ps). Other parameters used are $\tau_v = 20$ ps and $r_{Gd-O} = 3.1$ Å. For definitions of the dashed and dotted lines, see text.

electron spin relaxation is depicted in Figure 1b. Below 100 MHz there is an increase of r_1 observed with decreasing electron spin relaxation. At frequencies above 10 MHz the relaxivity maximum is however always limited by $\tau_R^{(2)}$.

In recent years it has been shown by various research groups (Kowalewski et al.,[22] Westlund et al.,[23,24] Sharp et al.,[25] and Fries et al.[20,21]) that electron relaxation due to static ZFS cannot be neglected in Gd(III) complexes, unlike in the SBM theory,[26] which only includes electron spin relaxation due to transient ZFS. Westlund[27] and Fries[28,29] have recently published complex analytical expressions for the proton spin relaxation that take both ZFS contributions into account. Fries and Belorizky[28] have shown that the longitudinal time correlation function of the spin $S = {}^7/_2$ of a Gd(III) complex has a quasi-monoexponential decay, and a simple analytical expression for the electron spin relaxation $1/T_{1e}$ can be found (eq 4). This simple analytical expression is valid if the Redfield−Abragam inequalities $a_2\tau_R^{(2)} \ll 1$ and $\omega_0 \gg a_2^2\tau_R^{(2)}$ are satisfied[30,31]

$$\frac{1}{T_{1e}} = \frac{12}{5}(a_{2T})^2\tau_v'\left(\frac{1}{1+\omega_S^2\tau_v'^2}+\frac{4}{1+4\omega_S^2\tau_v'^2}\right)+\frac{12}{5}(a_2)^2\tau_R^{(2)}\left(\frac{1}{1+\omega_S^2(\tau_R^{(2)})^2}+\frac{4}{1+4\omega_S^2(\tau_R^{(2)})^2}\right) \quad (4)$$

and

$$\frac{1}{\tau_v'} = \frac{1}{\tau_v}+\frac{1}{\tau_R^{(2)}} \qquad \frac{1}{\tau_{d1}} = \frac{1}{T_{1e}}+\frac{1}{\tau_R^{(2)}}$$

In eq 4 the magnitude of the transient and the static ZFS are characterized (in the second order) by a_{2T} and a_2, respectively. The second-order rotational correlation time $\tau_R^{(2)}$ is given by

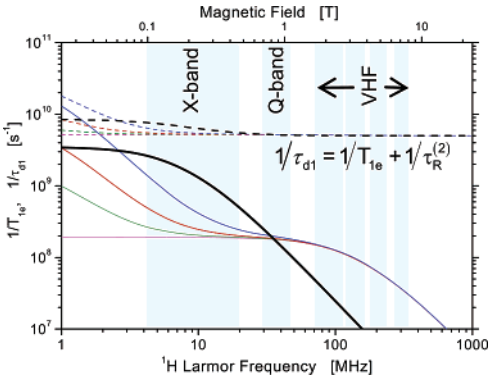

Figure 2. Longitudinal electron spin relaxation, $1/T_{1e}$ (full lines), and resulting correlation time for dipolar relaxation, $1/\tau_{d1}$ (dashed lines), as function of ^{1}H Larmor frequency. $1/T_{1e}$ and $1/\tau_{d1}$ calculated with SBM equation are shown in black ($a_{2T} = 0.4 \times 10^{10}$ s^{-1} and $\tau_v = 20$ ps); $1/T_{1e}$ and $1/\tau_{d1}$ calculated according to Fries and Belorizky are shown in color ($a_{2T} = 0.4 \times 10^{10}$ s^{-1}, $\tau_v = 1$ ps, and $a_2 = \{0.8, 0.4, 0.2, 0.0\} \times 10^{10}$ s^{-1} form top to bottom). The second-order rotational correlation time used is $\tau_R^{(2)} = 200$ ps, corresponding to small molecules.

$\tau_R^{(2)} = \tau_R/6$. Longitudinal electron spin relaxation rates $1/T_{1e}$ calculated with eq 4 using different a_2 values are compared in Figure 2 to those obtained by the SBM equation.

As pointed out by Fries and Belorizky[28] neglecting the static ZFS contribution is equivalent to assuming effective values for the transient ZFS amplitude: a_{2T} becomes $a_{2T}^{effective}$ and the correlation time τ_v becomes $\tau_v^{effective}$. While $a_{2T}^{effective}$ is expected to be similar to a_2 and a_{2T} (which often have comparable values), $\tau_v^{effective}$ should be intermediate between τ_v and $\tau_{(2)}$ (which can differ by several orders of magnitude). However, electronic relaxation rates $1/T_{1e}$ calculated with eq 4 (Figure 2, colored lines) differ substantially from those calculated with SBM theory and effective parameters (Figure 2, black lines).

As has been shown in Figure 1a relaxation of the proton spin is given by $J(\omega_I,\tau_{d1})$ and therefore depends on the dipolar correlation time τ_{d1} (eq 4). Above 30 MHz τ_{d1} is dominated by the rotational correlation time $\tau_R^{(2)}$ (at least for the model parameters chosen) and the proton relaxivity is not sensitive to a wrong theoretical model for the electron spin relaxation.

Relaxivities of macromolecular Gd(III) complexes with long rotational correlation times $\tau_R^{(2)}$ depend however on electron spin relaxation up to 100 MHz. Knowledge of the amplitudes of static (a_2, a_4, a_6) and transient (a_{2T}) ZFS is necessary for a full understanding of relaxivities at frequencies that are important for MRI. However, these amplitudes cannot be extracted from EPR spectra of such macromolecules because the line shapes are complex, and only extremely time-consuming numerical approaches are available, which preludes the fitting of extensive experimental data. We therefore propose to determine the ZFS parameters via multiple-frequency EPR on small Gd(III) complexes using the same chelating units. Parameters obtained in this way can then be used to evaluate proton nuclear magnetic relaxation dispersion (NMRD) profiles on macromolecular complexes, provided an adequate theoretical description is available.

Experimental Section

Materials. Synthesis of the monopropionate derivative of DTPA, H_5DTTA-Nprop, the bisamylamide derivative of EPTPA chelate H_3EPTPA-BAA,[11] the macrocyclic DOTA-like chelates, H_4TRITA,[9] H_3DO3APET, and H_3DO3APET$_2$,[12] as well as the

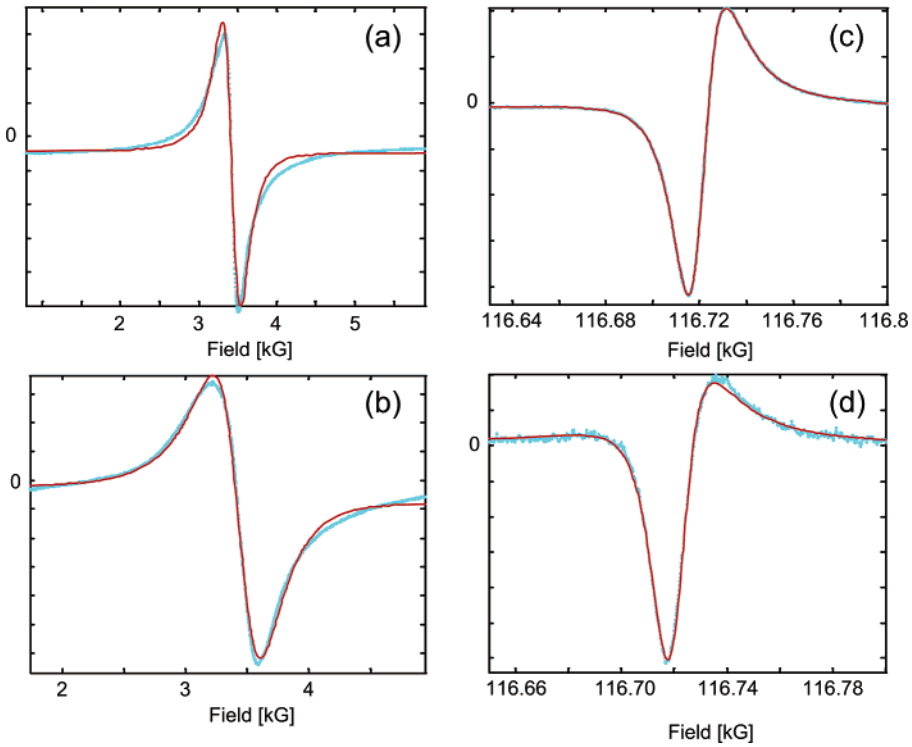

Figure 3. Experimental (red line) and underlying theoretical (blue dotted line) spectra for (a) [Gd(EPTPA-BAA)(H_2O)] and (b) [Gd(DTTA-Nprop)(H_2O)]$^{2-}$ both at X-band (9.43GHz), 25 °C, and (c) [Gd(EPTPA-BAA)(H_2O)] and (d) [Gd(DTTA-Nprop)(H_2O)]$^{2-}$ both at VHF (325.4 GHz), 12 °C. The spectra in parts a and b represent the best and worst cases of fitting a Lorentzian line to the experimental spectra. A difference of ~10% between the experimental and the extracted peak-to-peak width, ΔH_{pp}, is found in the worst case. The two spectra in parts c and d are out of phase due to the experimental setup, but the fits with the Lorentzian lines, taking into account the phases, are excellent. All ordinates are in arbitrary units.

cryptand ligands[13] CTBP and CTBPMe have been described previously. H_4TETA was purchased from commercial sources (Aldrich).

Sample Preparation. Solutions of [Gd(DTTA-Nprop)-(H_2O)]$^{2-}$ (49.4 mM), [Gd(EPTPA-BAA)(H_2O)] (43.4 mM), [Gd(TRITA)(H_2O)]$^{-}$ (33.3 mM), [Gd(TETA)]$^{-}$ (20.0 mM), [Gd(EPTPA)(H_2O)]$^{2-}$ (20.0 mM), [Gd(DO3APEt)(H_2O)]$^{-}$ and [Gd(DO3APEt$_2$)(H_2O)](4.9 and 4.2 mM, respectively) were prepared by mixing equimolar amounts of $Gd(ClO_4)_3$ and the ligand. A slight ligand excess (5%) was used, and the pH was adjusted to 6.0−6.5 by adding 0.1 M $HClO_4$ or 0.1 M NaOH. The sample solutions of [Gd(CTBP)($H_2O)_3$]$^{3+}$ and [Gd-(CTBPMe)($H_2O)_3$]$^{3+}$ were prepared by dissolution of trifluoroacetate solid complexes in double-distilled water (10.0 mM). All solutions were checked for the absence of free Gd(III) ion using the xylenol orange test.[14]

EPR Measurements. The EPR spectra at 120, 240, 218, and 325 GHz were measured at the EPR facility of the National High Magnetic Field Laboratory with home-built quasi-optical spectrometers. The measurements at 120 and 240 GHz were carried out on a superheterodyne spectrometer.[15] A configuration without a cavity was used with a Teflon sample cup containing approximately 40 μL of a solution of the Gd(III) complex. At 218 and 325 GHz, a homodyne spectrometer operating in reflection mode was used. The instrument is similar to that of Smith et al.,[16] with a 108.5 GHz Gunn diode as a microwave source and frequency multipliers allowing for 218 and 325 GHz.

Spectra at 75 and 225 GHz were obtained on a home-built spectrometer (Department of Experimental Physics, Technical University of Budapest, Hungary).[17] The 75 GHz Gunn oscillator is followed by a frequency tripler for the 225 GHz measurements. Poly(tetrafluoro ethylene) sample holders contain the aqueous samples that are placed in an oversized waveguide, so no resonant cavities are used.

W- (94 GHz), Q- (~34 GHz), and X-band (9.44 GHz) EPR spectra were recorded on Bruker ELEXSYS E680 (NHMFL) and E500 (EPFL) spectrometers, respectively. The microwave frequency was measured using a frequency counter embedded in the standard microwave bridge (W-, X-band) or an external Hewlett-Packard 5353B frequency counter (Q-band). Continuous-wave EPR was used at all frequencies.

Data Analysis. The peak-to-peak widths ΔH_{pp} and central fields B_c were determined by fitting the digitally recorded spectra to Lorentzian derivatives, with simultaneous baseline and phase correction (for examples see Figure 3).[18] These data were then analyzed within the framework of the Rast model (Supporting Information).[19−21] This model assumes that the electron spin relaxation is determined by the static or average ZFS up to the sixth order, which is modulated by molecular tumbling, and by the transient ZFS only up to the second order, which is modulated by random distortions of the complex. The least-squares fit procedure yields the following parameters:[19] The static ZFS magnitude parameters a_2, a_4, and a_6, the rotational correlation time at room temperature $\tau_R^{298} = 1/D_R{}^{298} = 6\tau_R^{(2),298}$, and its activation energy E_R, the transient ZFS magnitude a_{2T}, the associated correlation time $\tau_v{}^{298}$ and activation energy E_v, and the natural g-factor. To reduce the number of adjustable parameters, the rotational correlation time and its activation energy were fixed to the value obtained from ^{17}O measurements for all complexes. Furthermore, as the apparent g-factor converges toward its natural value with increasing frequency, the natural g-factor was fixed to its value at the highest available EPR frequency for each complex.

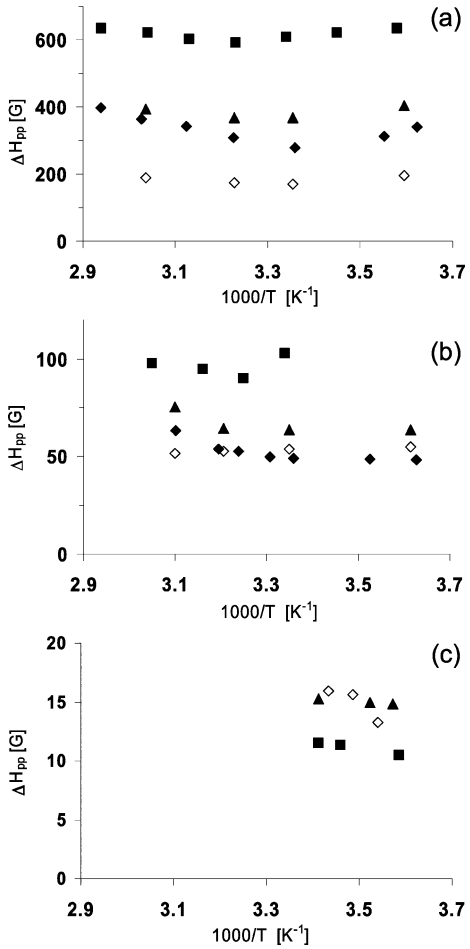

Figure 4. Temperature dependence of the peak-to-peak EPR linewidths, ΔH_{pp}, of Gd(III) acyclic polyaminocaroxylates compounds at (a) X-band, (b) Q-band, and (c) high frequencies (218 and 325 GHz): $[Gd(DTPA)(H_2O)]^{2-}$ (■) (at 325 GHz), $[Gd(EPTPA)(H_2O)]^{2-}$ (◆), [Gd(EPTPA-BAA)(H_2O)] (◇) (at 218 GHz), $[Gd(DTTA\text{-}Nprop)(H_2O)]^{2-}$ (▲) (at 218 GHz).

Results and Discussion

The peak-to-peak widths ΔH_{pp} and central fields B_c values were extracted from experimental EPR spectra using a single Lorentzian derivative.[18] At all EPR frequencies and for all complexes, the effective g-factor $g^{app} = \hbar\omega/\mu_B B_c$ were between 1.95 and 2.00. We observe for the four classes of complexes a considerable decrease of the ΔH_{pp} values with increasing frequency. However, temperature dependence of the peak-to-peak linewidths is small and shows no clear tendency for most of the complexes (Figures 4 and 5).

Experimental peak-to-peak widths of the acyclic compounds $[Gd(DTPA)(H_2O)]^{2-}$,$[Gd(DTTA\text{-}Nprop)(H_2O)]^{2-}$,$[Gd(EPTPA)(H_2O)]^{2-}$, and [Gd(EPTPA-BAA)$(H_2O)$] at X-band, Q-band, and very high frequency (VHF) are reported in Figure 4. At X-band, the peak-to-peak widths of the commercial acyclic contrast agent $[Gd(DTPA)(H_2O)]^{2-}$ are by far the largest ones.[21] At Q-band, the linewidths are drastically reduced with respect to X-band but remain notably larger compared to ΔH_{pp} of the other acyclic complexes. However, at VHF, the lines become much sharper, similar for all compounds, and comparable with those of macrocyclic complexes (Figure 4c).

Experimental peak-to-peak distances of the macrocyclic polyaminocarboxylates and the cryptand compounds $[Gd(DOTA)(H_2O)]^-$,$[Gd(TRITA)(H_2O)]^-$,$[Gd(TETA)]^-$,$[Gd(DO3APEt)(H_2O)]^-$, $[Gd(DO3APEt_2)(H_2O)]$, $[Gd(CTBP)(H_2O)_3]^{3+}$, and $[Gd(CTBPMe)(H_2O)_3]^{3+}$ are reported in Figure 5. At X-band, the commercial macrocyclic contrast agent $[Gd(DOTA)(H_2O)]^-$ has the lowest ΔH_{pp} value.[19] As was the case for the acyclic complexes, the differences in ΔH_{pp} between the complexes are reduced when the EPR frequencies augment. At VHF, the linewidths of most complexes decrease and become very similar. The DOTA-like $[Gd(TETA)]^-$ has a different EPR relaxation behavior. It has by far the largest ΔH_{pp} value at Q-band and an opposite temperature dependence of the peak-to-peak linewidths.

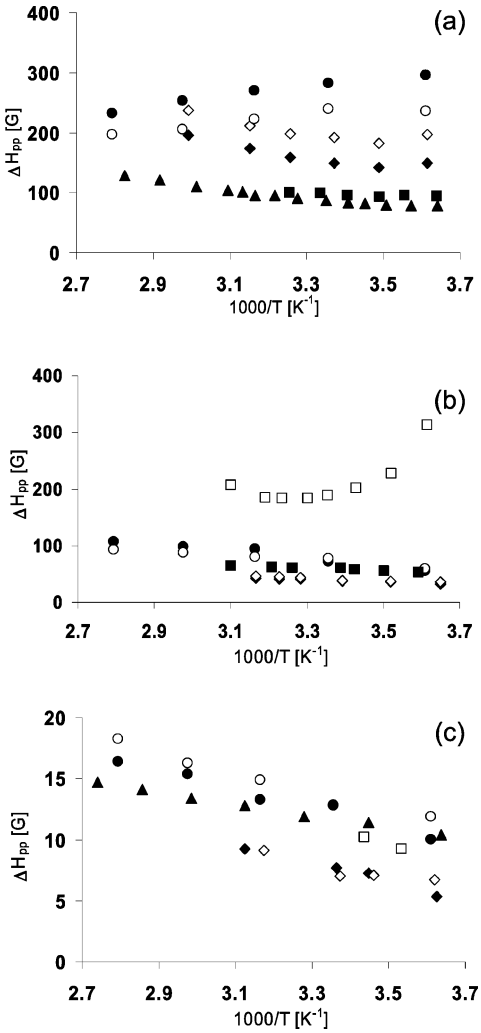

Figure 5. Temperature dependence of the peak-to-peak EPR linewidths, ΔH_{pp}, of Gd(III) macrocyclic polyaminocarboxylates and cryptand compounds at (a) X-band, (b) Q-band, and (c) high frequencies (225, 240, and 325 GHz): $[Gd(DOTA)(H_2O)]^-$ (▲) (at 225 GHz), $[Gd(TRITA)(H_2O)]^-$ (■),$[Gd(TETA)]^-$ (□)(at325GHz),$[Gd(DO3APEt)(H_2O)]^-$ (◆) (at 240 GHz), $[Gd(DO3APEt_2)(H_2O)]$ (◇) (at 240 GHz), $[Gd(CTBP)(H_2O)_3]^{3+}$ (○) (at 225 GHz), $[Gd(CTBPMe)(H_2O)_3]^{3+}$ (●) (at 225 GHz).

Acyclic Polyaminocarboxylate Complexes. The results of the analysis of the EPR data (Figure 6) using the model of Rast−Fries,[21] which includes the static and transient ZFS for the three acyclic complexes are reported in Table 1.

The theoretical curves and the experimental data for $[Gd(DTTA\text{-}Nprop)(H_2O)]^{2-}$ and [Gd(EPTPA-BAA)(H_2O)] are shown in Figure 6. The peak-to-peak widths for both complexes are well reproduced at all frequencies. However, we noticed a non-negligible discrepancy between the theoretical curves and the experimental data at X-band for the apparent g-factors. The first possible explanations could be that the ZFS Hamiltonian is not negligible in comparison with the Zeeman Hamiltonian at low magnetic fields (typically 1000−5000 G for X-band). It has been

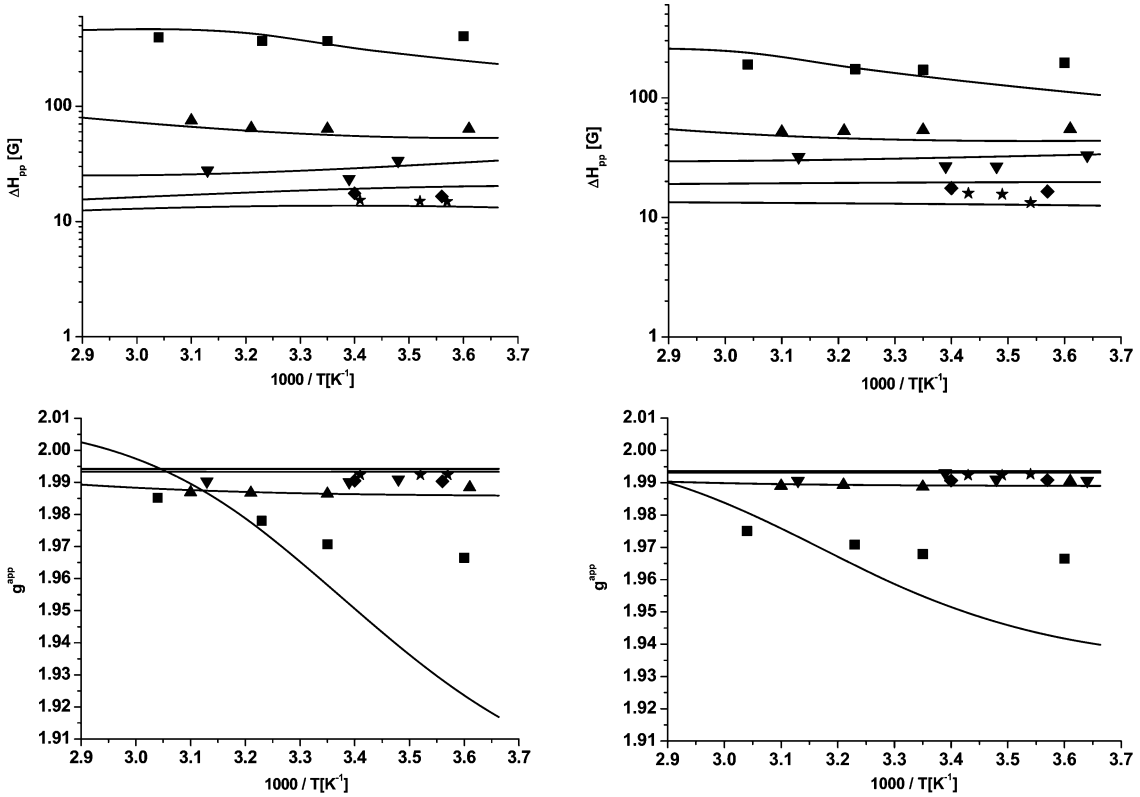

Figure 6. Experimental and theoretical EPR peak-to-peak widths and apparent *g*-factors for aqueous solutions of $[Gd(DTTA\text{-}Nprop)(H2O)]^{2-}$ (left) and $[Gd(EPTPA\text{-}BAA)(H_2O)]$ (right) at X-band (■), Q-band (▲), W-band (▼), 218 (◆), and 325 GHz (★). Theoretical curves are represented as full lines.

TABLE 1: Electron Spin Relaxation Parameters of Gd(III) Complexes Obtained from the Analysis of Peak-to-Peak Widths and Central Fields[a]

ligand	DTPA[b]	DTTA -Nprop	EPTPA-BAA	DOTA[c]	DO3APEt	$DO3PEt_2$	CTBP	CTBPMe
$a_2/10^{10}$ s^{-1}	0.92	0.35	0.31	0.35	0.52	0.60	0.09	
$a_4/10^{10}$ s^{-1}		0	0		0	0	0	
$a_6/10^{10}$ s^{-1}		0.02	0.01		0	0	0.011	0.06
$a_{2T}/10^{10}$ s^{-1}	0.43	0.56	0.56	0.43	0.36	0.35	0.47	0
$\tau_R^{298}/10^{-12}$ s	395	*642*[d]	*1190*[d]	491	*500*[e]	*550*[e]	*600*[f]	*643*[f]
E_R/kJ mol^{-1}	12.6	*16*[d]	*18*[d]	16.4	*17*[e]	*18*[e]	*18*[f]	*18*[f]
$\tau_v^{298}/10^{-12}$ s	1.33	0.26	0.35	0.54	0.77	0.80	0.73	0.75
E_v/kJ mol^{-1}	15.7	9	8	6.0	6.0	6.0	6.0	6.0
g		1.994	1.993	1.992	1.990	1.990	1.992	1.992

[a] Italic values were fixed during the least-squares adjustment. [b] Reference 21. [c] Reference 19. [d] Reference 11. [e] Reference 12. [f] Reference 13.

shown using Monte Carlo (MC) simulations[32] that for small complexes, such as, for example, $[Gd(DOTA)(H_2O)]^-$, even at low temperatures (i.e., long τ_R) there is no severe violation of this approximation. However, these remaining small violation effects can be the source of the discrepancy observed at low frequencies. A way to check this explanation could be the use of this particular approach (MC simulations) to calculate high-resolution derivative EPR spectra, but this would be extremely time-consuming. A second explanation could be a significant source of uncertainty from the extraction of the central fields, especially at X-band where fitting broad experimental spectra as a single Lorentzian derivative is not sufficiently accurate to achieve a reasonable determination of the central field B_c.

The static ZFS parameters a_2 for $[Gd(DTTA\text{-}Nprop)(H_2O)]^{2-}$ and $[Gd(EPTPA\text{-}BAA)(H_2O)]$ are 3 times lower than those for $[Gd(DTPA)(H_2O)]^{2-}$ [21] (Table 1). This was of course expected from the X-band EPR linewidths, where the static ZFS modulation process plays a dominant role.[19,21] The obtained values of the fourth order a_4 are negligible. But, the influence of the sixth-order static ZFS parameter a_6 was significant for both complexes and was taken into account for a better fit. The transient ZFS parameters a_{2T} seem to remain essentially the same for all acyclic complexes. The values of the vibrational activation energy E_v are reasonable and very similar to those calculated by a simultaneous NMRD, ^{17}O, and EPR analysis. The values calculated for the vibrational correlation time, τ_v, are quite short. This is a consequence of the moderate peak-to-peak widths observed at VHF. Although the lines are much sharper than at X-band, ΔH_{pp} remains on the order of a few Gauss. If we use a longer τ_v value, then the calculated linewidth becomes exceedingly small at such high magnetic fields and EPR frequencies, due to the decay proportional to ω_S^{-2} of the spectral densities when $\omega_S\tau_v \gg 1$. Thus, the slow decrease of the observed peak-to-peak widths with increasing frequency (above W-band) cannot be reproduced using a longer τ_v.

Macrocyclic Polyaminocarboxylate Complexes. The results obtained for the two macrocyclic DOTA-like phosphinate complexes are reported in Figure 7. As for acyclic complexes, we notice that it is more difficult to obtain a satisfactory fit for the X-band experimental data than for higher frequencies for the apparent *g*-factors. The fitting results of the whole set of experimental spectra at X-band, Q-band, and VHF are reported

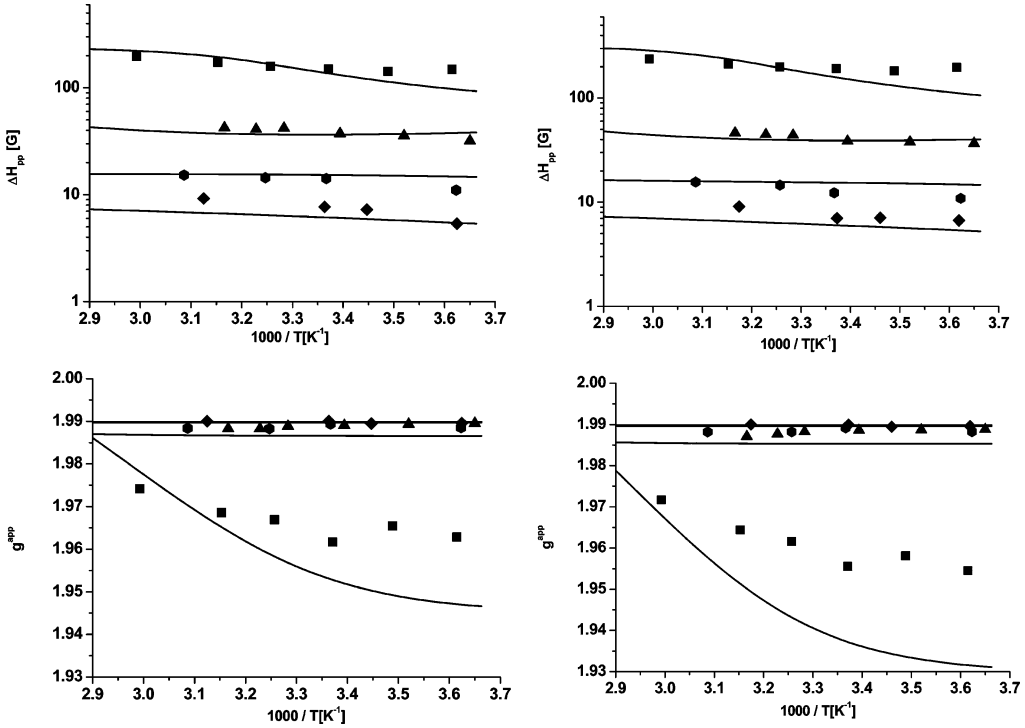

Figure 7. Experimental and theoretical EPR peak-to-peak widths and apparent *g*-factors for aqueous solutions of $[Gd(DO3APEt)(H_2O)]^-$ (left) and $[Gd(DO3APEt_2)(H_2O)]$ (right) at X-band (■), Q-band (▲), 120 GHz (⬢), and 240 GHz (◆). Theoretical curves are represented as full lines.

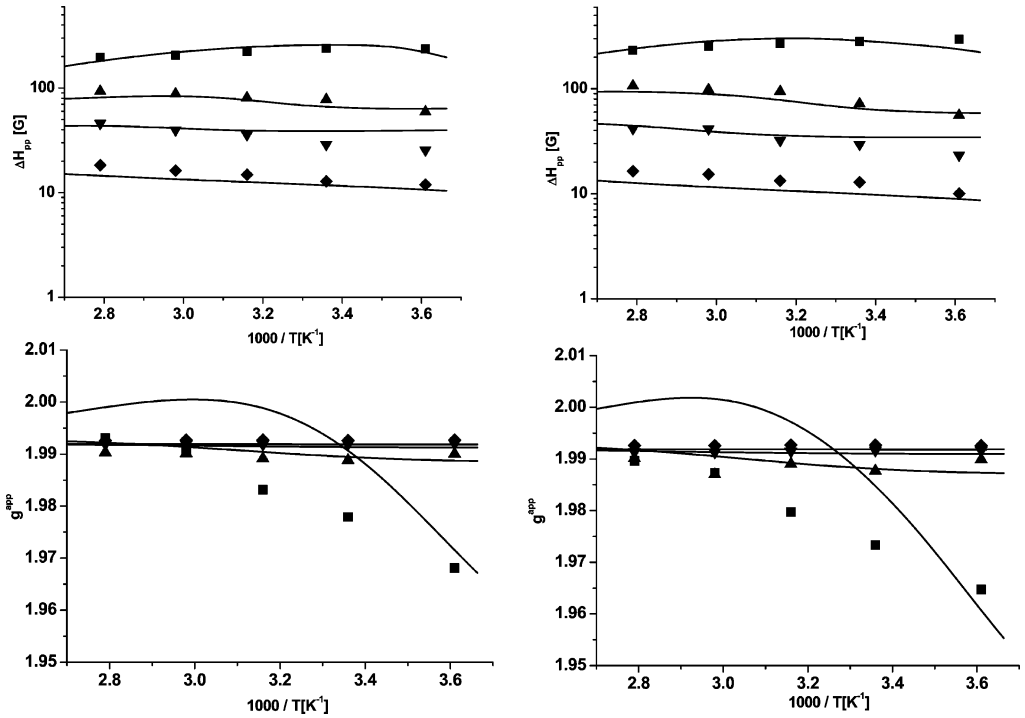

Figure 8. Experimental and theoretical EPR peak-to-peak widths and apparent *g*-factors for aqueous solutions of $[Gd(CTBP)(H_2O)_3]^{3+}$ (left) and $[Gd(CTBPMe)(H_2O)_3]^{3+}$ (right) at X-band (■), Q-band (▲), 75 (▼), and 225 GHz (◆). Theoretical curves are represented as full lines.

in Table 1. The values of the static ZFS parameter a_2 are close for $[Gd(DO3APEt_2)(H_2O)]$ and $[Gd(DO3APEt)(H_2O)]^-$ and about 2 times larger than those for $[Gd(DOTA)(H_2O)]^-$. The magnitudes of a_4 and a_6 are very small when we let all ZFS parameters freely vary. Therefore, we set $a_4 = a_6 = 0$ in the final adjustments.

Cryptand Complexes. The cryptand-based complexes $[Gd(CTBP)(H_2O)_3]^{3+}$ and $[Gd(CTBPMe)(H_2O)_3]^{3+}$ behave differently in comparison to the polyaminocarboxylate-based ones. At X-band ΔH_{pp} values decrease with temperature (Figure 5a). At higher EPR frequencies the temperature dependency reverses and becomes similar to that found for the other complexes. The data analysis reveals for both cryptands very small values of a_2, negligible values for a_4, and significant values for a_6 (Table 1 and Figure 8). Fixing the higher-order term a_6 to zero leads to an opposite temperature dependence at X-band (Supporting Information). Similar values for a_2 and a_6 have been obtained for the eight-coordinate Gd(III) aqua ion (0.0946 and 0.0232, respectively, from simultaneous analysis of EPR, ^{17}O NMR, and ^1H NMRD data).[33]

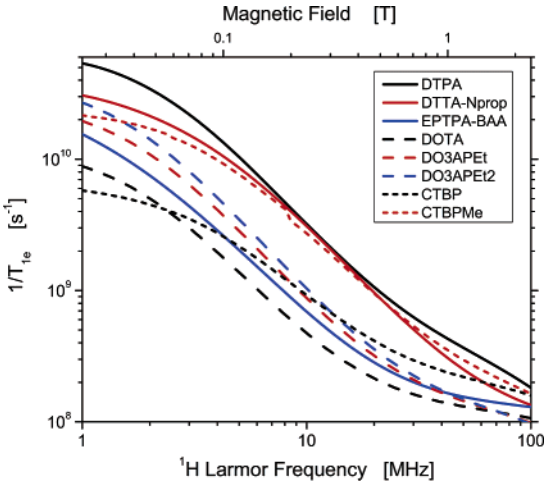

Figure 9. Longitudinal electron spin relaxation, $1/T_{1e}$, calculated for $[Gd(L)(H_2O)]^{n-/+}$ in aqueous solution according to Fries and Belorizky (refs 28 and 29, including a sixth-order term for static ZFS) and parameters in Table 1.

Electronic Relaxation and Relaxivity. Longitudinal electron spin relaxation rates, $1/T_{1e}$, can be easily calculated from the parameters in Table 1 using the analytical equations derived by Fries and Belorizky (Figure 9, for the equations see the Supporting Information).[28,29] In accordance with the estimation using the SBM theory shown in Figure 2, $1/T_{1e}$ values decrease strongly with increasing magnetic field strength. For the complexes studied the electronic relaxation at low magnetic fields ($\nu_I < 10$ MHz) is dominated by the static ZFS and varies substantially between complexes with different chelating ligands. At proton Larmor frequencies above 60 MHz $1/T_{1e}$ values are $<3 \times 10^8$ s^{-1} for all complexes studied. At these frequencies the transient ZFS is dominating the longitudinal electronic relaxation of the small complexes considered here ($\tau_R^{(2)} = \tau_R/6 < 200$ ps).

Among the acyclic complexes [Gd(EPTPA-BAA)(H_2O)] has the slowest electron spin relaxation. Thus, besides its favorable water exchange ($k_{ex}^{298} = 57 \times 10^6$ s^{-1})[11] this compound also has a favorable electronic relaxation, compared to that of the DTPA complex, for example. Both macrocyclic polyaminocarboxylate complexes with a phosphonate group, DO3APEt and DO3APEt_2, have faster electron spin relaxation compared to that of the DOTA complex. This faster relaxation corresponds to a higher $1/T_{1e}^{static}$ value, which is caused by larger a_2 values (Table 1). Interestingly, for the cryptand ligands CTBP and CTBPMe the static ZFS is dominated by the sixth-order term, a_6. From the analytical equations for $1/T_{1e}$ of Belorizky and Fries[28] the following approximations for $1/T_{1e}^{static}$ can be derived at low (eq 5) and high (eq 6) frequencies

$$\frac{1}{T_{1e}^{static}} \simeq \left(2(a_2)^2 + \frac{440}{7}(a_4)^2 + 900(a_6)^2\right)\tau_R \text{for}$$

$$(k\omega_S\tau_R^{(k)})^2 \ll 1 \quad k = 2,4,6 \quad (5)$$

$$\frac{1}{T_{1e}^{static}} \simeq \left(\frac{144}{5}(a_2)^2 + \frac{70'400}{21}(a_4)^2 + \frac{1'360'800}{13}(a_6)^2\right)\frac{1}{\omega_S{}^2\tau_R}$$

$$(\text{for} k\omega_S\tau_R^{(k)})^2 \gg 1 \quad k = 2,4,6 \quad (6)$$

The weight of the sixth-order term is always much higher than that of the second-order term, explaining why even small a_6 values can be important for the overall static ZFS relaxation.

At higher magnetic fields the transient ZFS contribution to electronic relaxation becomes increasingly important (Figure 10, left panel). At a proton frequency of 64 MHz ($B = 1.5$ T) $1/T_{1e}^{transient}$ is more than 3 times larger than $1/T_{1e}^{static}$ for most of the complexes considered. No simple correlation between the structures of chelating ligands and parameters defining $1/T_{1e}^{transient}(a_{2T},\tau_v)$ could be found. In contrast to the rather strong dependence of the static ZFS on the nature of the chelating ligand not much dependence is observed for the transient ZFS. The electronic relaxations of Gd(III) complexes considered are compared in Figure 10 (right) at two high magnetic field strengths used in modern MRI instruments (1.5 and 3.0 T, corresponding to resonance frequencies of 42 and 84 GHz and 64 and 128 MHz for EPR and NMR, respectively).

It is observed that the variation of electronic relaxation between different complexes decreases with increasing magnetic field. The order of $1/T_{1e}$ observed for different complexes can even change by increasing the magnetic field, as, for example, for the very similar cryptand complexes. Nevertheless, we would like to mention again that for the relatively fast rotating complexes studied here longitudinal NMR relaxivity at frequencies above ~70 MHz is dominated by the rotational correlation time and therefore independent of $1/T_{1e}$. However, by binding these complexes to macromolecules the rotational correlation times become much longer, and therefore the electron spin relaxation contributions will no longer be negligible.

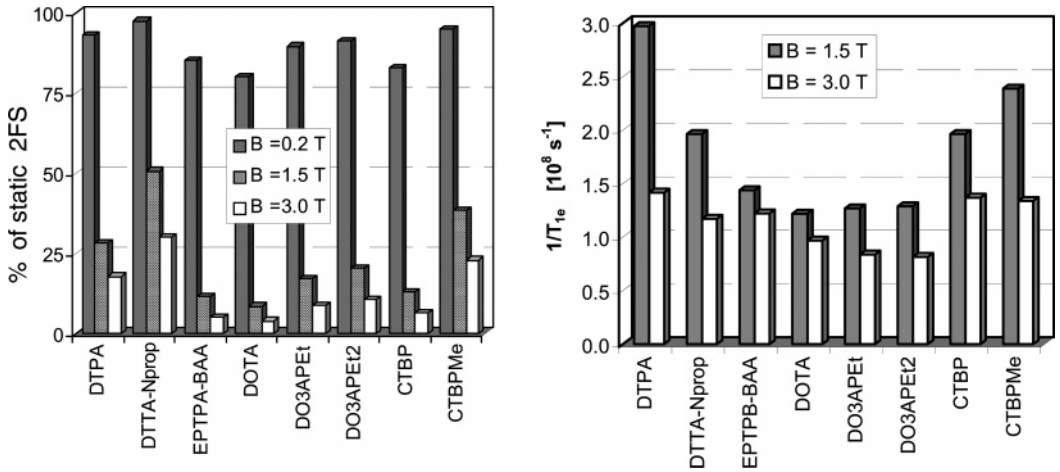

Figure 10. Left panel: Contribution of $1/T_{1e}^{static}$ to the overall electronic relaxation $1/T_{1e}$ for increasing magnetic field *B*. Right panel: longitudinal electron spin relaxation, $1/T_{1e}$, calculated using parameters in Table 1 for $[Gd(L)(H_2O)]^{n-}$ in aqueous solution at 1.5 and 3.0 T.

Conclusions

In this paper we report parameters for static and transient ZFS determined from EPR spectra of relatively small and therefore fast rotating Gd(III) complexes. A strong decrease of the linewidths, expressed as ΔH_{pp}, has been observed with increasing EPR frequency, whereas the temperature dependences of ΔH_{pp} found are in general weak. Besides this general observation we found that at X-band ΔH_{pp} differs substantially between different Gd(III) complexes. At high frequencies however the linewidths are nearly independent of the nature of the chelating ligand.

For the compounds studied static ZFS interaction is dominating longitudinal electronic relaxation $1/T_{1e}$ at low magnetic fields ($B < 0.2$ T). At high magnetic fields ($B > 1.5$ T) $1/T_{1e}$ is dominated by the transient ZFS interaction. A marked dependence has been found between the nature of chelating ligand of the coordination environment of Gd(III) and the parameters (a_2, a_6) defining static ZFS $1/T_{1e}^{static}$. For the transient ZFS interaction the differences found for the Gd(III) complexes studied are much less pronounced than those for the static ZFS. No explanation can be given at the moment for how molecular vibrations and impacts of solvent molecules influence $1/T_{1e}^{transient}$. However, at high field these contributions dominate the longitudinal electronic relaxation, and thus the longitudinal relaxation rates do not depend much on the nature of the ligand.

Water proton spin relaxivities r_1 have been calculated as a function of resonance frequency with ZFS parameters determined using recent analytical expressions for $1/T_{1e}$. It could be shown that for the relatively fast rotating molecules such as $[Gd(DOTA)(H_2O)]^-$ and $[Gd(DTPA)(H_2O)]^{2-}$ relaxivity is mainly limited by the fast rotation and that electronic relaxation has only a marked influence at frequencies below 30 MHz. For slower rotating complexes the influence of $1/T_{1e}$ on relaxivity extends however to higher frequencies, and using chelates with slow electronic spin relaxation will lead to higher r_1 values. Electronic relaxation will have no influence on the efficiency of MRI contrast agents designed for studies at very high magnetic fields.

Acknowledgment. We thank Drs. J. van Tol, A. Ozarowski and L.-C. Brunel (National High Magenetic Field Laboratory, Tallahassee, FL) for their assistance during the high-frequency EPR experiments as well as for the valuable advice and discussions. We also thank Petra Lebdušková (Ecole Polytechnique Fédérale de Lausanne) for preparing the $[Gd(DO3APEt_2)(H_2O)]$ and $[Gd(DO3APEt)(H_2O)]^-$ samples. This work is supported by the Swiss National Science Foundation and the Swiss State Secretariat for Education and Research. This research was carried out within EU COST Action D18 and the European-founded EMIL program (LSHC-2004-503569).

Supporting Information Available: Tables of experimental EPR data, figures of longitudinal electron spin relaxations and multifrequency experimental and theoretical peak-to-peak widths and apparent *g*-factors for $[Gd(CTBP)(H_2O)_3]^{3+}$ $[Gd(CTBPMe)(H_2O)_3]^{3+}$, a theoretical description of the Rast−Borel model, experimental and fitted spectra at 9.44 GHz (25 °C) and at 3 25.4 GHz (12 °C) of $[Gd(DTTA\text{-}Nprop)(H_2O)]^{2-}$ and [Gd(EPTPA-BAA)(H_2O)]. This material is available free of charge via the Internet at http://pubs.acs.org.

References and Notes

(1) Caravan, P.; Ellison, J. J.; McMurry, T. J.; Lauffer, R. B. *Chem. Rev.* **1999**, *99*, 2293.
(2) Tóth, É.; Helm, L.; Merbach, A. E. *Top. Curr. Chem.* **2002**, *221*, 61.
(3) Borel, A.; Tóth, É.; Helm, L.; Jánossy, A.; Merbach, A. E. *Phys. Chem. Chem. Phys.* **2000**, *2*, 1311.
(4) Clarkson, R. B.; Smirnov, A. I.; Smirnova, T. I.; Kang, H.; Belford, R. L.; Earle, K.; Freed, J. H. *Mol. Phys.* **1998**, *96*, 1325.
(5) Powell, D. H.; Merbach, A. E.; Gonzalez, G.; Brücher, E.; Micskei, K.; Ottaviani, M. F.; Köhler, K.; von. Zelewsky, A.; Grinberg, O. Y.; Lebedev, Y. S. *Helv. Chim. Acta* **1993**, *76*, 2129.
(6) Laus, S.; Ruloff, R.; Tóth, É.; Merbach, A. E. *Chem.—Eur. J.* **2003**, *9*, 3555.
(7) Tóth, É.; Helm, L.; Kellar, K. E.; Merbach, A. E. *Chem.—Eur. J.* **1999**, *5*, 1202.
(8) Nicolle, G. M.; Tóth, É.; Schmitt-Willich, H.; Raduchel, B.; Merbach, A. E. *Chem.—Eur. J.* **2002**, *8*, 1040.
(9) Ruloff, R.; Tóth, É.; Scopelliti, R.; Tripier, R.; Handel, H.; Merbach, A. E. *Chem. Commun.* **2002**, *22*, 2630.
(10) Laus, S.; Sour, A.; Ruloff, R.; Tóth, E.; Merbach, A. E. *Chem.—Eur. J.* **2005**, *11*, 3064.
(11) Jaszberenyi, Z.; Sour, A.; Tóth, É.; Benmelouka, M.; Merbach, A. E. *Dalton Trans.* **2005**, *16*, 2713.
(12) Lebdušková, P.; Hermann, P.; Helm, L.; Tóth, É.; Kotek, J.; Lukeš, I.; Merbach, A. E., submitted for publication.
(13) Burai, L.; Tóth, É.; Bazin, H.; Benmelouka, M.; Jászberényi, Z.; Helm, L.; Merbach, A. E. *Dalton Trans.* **2006**, 629.
(14) Brunisholz, G.; Randin, M. *Helv. Chim. Acta.* **1959**, *42*, 1927.
(15) van Tol, J.; Brunel, L.C.; Wylde, R.J. *Rev. Sci. Instrum.* **2005**, *76*, 074101.
(16) Smith, G. M.; Lesurf, J. C. G.; Mitchell, R. H.; Riedi, P. C. *Rev. Sci. Instrum.* **1998**, *69*, 3924.
(17) Fehér, T. Diploma Work, Technical University of Budapest, Budapest, Hungary, 1997.
(18) Helm, L.; Borel, A. *NMRICMA*, version 2.7; Ecole Polytechnique Fédérale de Lausanne: Lausanne, Switzerland, 2000.
(19) Rast, S.; Borel, A.; Helm, L.; Belorizky, E.; Fries, P. H.; Merbach, A. E. *J. Am. Chem. Soc.* **2001**, *123*, 2637.
(20) Rast, S.; Fries, P. H.; Belorizky, E. *Mol. Phys.* **1999**, *96*, 1543.
(21) Rast, S.; Fries, P. H.; Belorizky, E. *J. Chem. Phys.* **2000**, *113*, 8724.
(22) Kowalewski, J.; Nordenskiöld, L.; Benetis, N.; Westlund, P.-O. *Prog. Nucl. Magn. Reson. Spectrosc.* **1985**, *17*, 141.
(23) Strandberg, E.; Westlund, P.-O. *J. Magn. Reson., Ser. A* **1996**, *122*, 179.
(24) Strandberg, E.; Westlund, P.-O. *J. Magn. Reson.* **1999**, *137*, 333.
(25) Abernathy, S. M.; Sharp, R. R. *J. Chem. Phys.* **1997**, *106*, 9032.
(26) (a) Solomon, I.; Bloembergen, N. *J. Chem. Phys.* **1956**, *25*, 261. (26) (b) Bloembergen, N.; Morgan, L. O. *J. Chem. Phys.* **1961**, *34*, 842.
(27) Zhou, X.; Westlund, P. *Spectrochim. Acta, Part A* **2005**, *62*, 76.
(28) Belorizky, E.; Fries, P. H. *Phys. Chem. Chem. Phys.* **2004**, *6*, 2341.
(29) Fries, P. H.; Belorizky, E. *J. Chem. Phys.* **2005**, *123*, 124510.
(30) Redfield, A. G. The Theory of Relaxation Processes In *Advances in Magnetic Resonance*; Waugh, J. S., Ed.; Academic Press: New York, 1965; Vol. 1, p 1.
(31) Abragam, A. *The Principles of Nuclear Magnetism*; Clarendon Press: Oxford, U. K., 1961; p 281.
(32) Rast, S.; Fries, P. H.; Belorizky, E.; Borel, A.; Helm, L.; Merbach, A. E. *J. Phys. Chem.* **2001**, *115*, 7554.
(33) Borel, A.; Yerly, F.; Helm, L.; Merbach, A. E. *J. Am. Chem. Soc.* **2002**, *124*, 2042.